Acta Pharmacologica Sinica (2014) 35: 1546–1555
 1671-4083/14 $32.00
www.nature.com/aps

Original Article

G226, a new epipolythiodioxopiperazine derivative, triggers DNA damage and apoptosis in human cancer cells *in vitro* via ROS generation

Peng-xing HE[1, #], Jie ZHANG[3, #], Yong-sheng CHE[2], Qiao-jun HE[1], Yi CHEN[3, *], Jian DING[3, *]

[1]Institute of Pharmacology and Toxicology, School of Pharmaceutical Sciences, Zhejiang University, Hangzhou 310058, China; [2]Beijing Institute of Pharmacology & Toxicology, Beijing 100190, China; [3]Division of Anti-tumor Pharmacology, State Key Laboratory of Drug Research, Shanghai Institute of Materia Medica, Chinese Academy of Sciences, Shanghai 201203, China

Aim: G226 is a novel derivative of epipolythiodioxopiperazines with potent inhibitory activity against cancer cells. Here, we sought to identify potential targets involved in the anti-cancer activity of G226.
Methods: Cell proliferation assay was conducted in a panel of 12 human cancer cell lines. The activities of topoisomerase I (Topo I) and Topo II were studied using supercoiled pBR322 DNA relaxation and kDNA decatenation assays. ROS production was assessed with probes DCFH-DA and H&E. Western blot analysis and flow cytometry were used to examine DNA damage, apoptosis and cell cycle changes.
Results: G226 displayed potent cytotoxicity in the 12 human cancer cell lines with a mean IC_{50} value of 92.7 nmol/L. This compound (1–100 μmol/L) selectively inhibited the activity of Topo II, and elevated the expression of phosphorylated-H2AX in a dose-dependent manner. In Topo II-deficient HL60/MX2 cells, however, G226-induced DNA damage, apoptosis and cytotoxicity were only partially reduced, suggesting that Topo II was not essential for the anti-tumor effects of G226. Furthermore, G226 (0.125–2 μmol/L) dose-dependently elevated the intracellular levels of H_2O_2 and $O_2^{\cdot-}$ in the cancer cells, and pretreatment with GSH, NAC or DTT not only blocked G226-induced intracellular accumulation of ROS, but also abrogated G226-mediated phosphorylation of H2AX, apoptosis and cytotoxicity.
Conclusion: G226-mediated ROS production contributes to the anti-cancer activity of this compound.

Keywords: G226; epipolythiodioxopiperazine; 11′-deoxyverticillin A; anti-cancer agent; Topo II; DNA damage; apoptosis; ROS; antioxidant

Acta Pharmacologica Sinica (2014) 35: 1546–1555; doi: 10.1038/aps.2014.105

Introduction

DNA topoisomerase II (Topo II) is a nuclear enzyme that corrects topological DNA errors in replication, transcription, recombination, and chromosome condensation and decondensation via a DNA breakage/reunion mechanism[1]. Although the biological functions of Topo II are important for ensuring genomic integrity, the ability to interfere with Topo II and generate enzyme-mediated DNA damage is an effective strategy for cancer chemotherapy[2, 3]. In fact, most clinically active agents including etoposide, doxorubicin, and mitoxantrone are Topo II inhibitors, which induce DNA strand breaks, thereby causing apoptosis.

# These authors contributed equally to this work.
* To whom correspondence should be addressed.
E-mail jding@simm.ac.cn (Jian DING);
ychen@simm.ac.cn (Yi CHEN)
Received 2014-05-15 Accepted 2014-08-29

Reactive oxygen species (ROS), such as the free radical superoxide radical ($O_2^{\cdot-}$), the hydroxyl free radical ($HO^{\cdot}$), and the non-radical hydrogen peroxide (H_2O_2), are unstable metabolites of molecular oxygen and associated with nearly all bodily processes[4]. Under physiological conditions, a certain level ROS acts as an important signaling molecule, which plays a role in the regulation of other important processes through modulation of signal pathways, thereby influencing the synthesis of antioxidant enzymes, repair processes, inflammation, and cell proliferation[5, 6]. However, high levels of ROS lead to apoptosis and necrosis, which are implicated in cancer, aging, and neurodegenerative disorders[7, 8]. Although ROS are maintained at low levels via various enzyme systems participating in the *in vivo* redox homeostasis, many factors, including endogenous biological or exogenous environmental factors, can induce an imbalance between the pro-oxidants and antioxidants or alter enzyme activity, as observed with

chemical exposure, drugs, pollution, or radiation[4]. ROS have also been implicated in the antitumor effects of some anticancer drugs[9, 10]. A number of anticancer drugs produce ROS at various cellular sites *in vivo*.

Epipolythiodioxopiperazines (ETPs) are produced by fungi, and recent studies have highlighted the potential of ETPs as anticancer agents[11]. Many studies have shown that ETPs exert anti-tumor effects through inhibition of cancer cell growth, induction of apoptosis, and autophagy[12], inhibition of DNA topoisomerase activity[13], antiangiogenesis[14], and induction of ROS[11]. G226 is a novel ETP that was synthesized by replacing methyl with acetyl at point 13 of 11′-deoxyverticillin A (Figure 1). In previous studies, we have reported that G226 exhibits potent cytotoxic activity against breast cancer cells. This agent also displays remarkable apoptosis-inducing effects, which were shown to be caspase 8-dependent. Additionally, G226 triggers autophagy. Upregulated LC3 and p62 were co-localized with caspase 8, which mediated caspase 8 activation and apoptosis induction. Our group has continued to study the anti-tumor mechanism of this compound. In the current study, we investigated whether G226 altered ROS and inhibited Topo II activity, analyzed the function of ROS in G226-induced DNA damage, and determined the role that ROS play in the anti-tumor activity of G226.

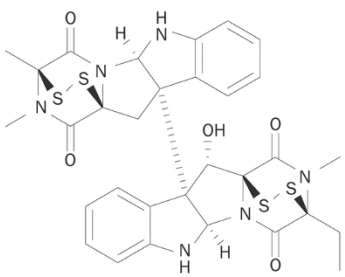

Figure 1. Chemical structure of G226.

Materials and methods

Chemicals

G226 was kindly provided by Prof Yong-sheng CHE (Beijing Institute of Pharmacology & Toxicology, Beijing, China). The purity of the compound was greater than 98%. Adriamycin (ADR), etoposide (VP16), camptothecin (CPT), 7-ethyl-10-hydroxycamptothecin (SN38), 2,7-dichlorodihydro fluorescein diacetate (DCFH-DA), and hydroethidine (HE) were purchased from Sigma (St Louis, MO, USA). All of the above compounds were dissolved in DMSO at 10 mmol/L (used *in vitro*) as a stock solution and stored at -20 °C. Glutathione (GSH), N-acetylcysteine (NAC), and dithiothreitol (DTT) were purchased from Beyotime (Nantong, China), dissolved in sterile water at 100 mmol/L as a stock solution and stored at 4 °C. All compounds were diluted to the desired concentration immediately before each experiment, and the final DMSO concentrations did not exceed 0.1%.

Cell culture

Human promyelocytic leukemia HL-60 and HL-60/MX2, lung adenocarcinoma A549 and H1975, breast carcinoma BT474, colorectal adenocarcinoma HT-29 and HCT-116 cell lines were obtained from the American Type Culture Collection (ATCC, Manassas, VA, USA). Human gastric adenocarcinoma MKN-1 and MKN-45 cells and the ovarian epithelioid carcinoma SK-OV-3 cell lines were obtained from the Japanese Foundation of Cancer Research (Tokyo, Japan). The human hepatocellular carcinoma BEL-7402 and SMMC-7721, the ovarian epithelioid carcinoma HO-8910, bladder carcinoma T-24, and lung adenocarcinoma H460 cell lines were obtained from the Cell Bank of the Shanghai Institute of Materia Medica, Chinese Academy of Sciences. HL-60, HL-60/MX2, H1975, MKN-1, MKN-45, BEL-7402, SMMC-7721, HO-8910, and H460 cell lines were maintained in RPMI-1640 medium (Gibco, Grand Island, NY, USA). BT474 and SK-OV-3 cells were maintained in LG-DMEM medium (Gibco). Finally, HCT-116, HT-29, and T-24 cells were maintained in McCoy's 5A medium (Gibco), whereas A549 cells were maintained in F12 medium (Gibco). All cells were supplemented with 10% heat-inactivated fetal calf serum (FBS; Gibco) at 37 °C in a 5% CO_2 humidified environment.

Cell proliferation assay

The cytotoxic characteristics of G226 were examined in a panel of human tumor cell lines, applying ADR as reference compound. Cells in 96-well plates were treated with gradient concentrations of the compounds at 37 °C for 72 h. Cell proliferation was determined using sulforhodamine B (SRB; Sigma, St Louis, MO, USA). The cytotoxicity of G226 against HL-60 and HL-60/MX2 cells was determined using CCK-8 (Dojindo laboratories, Kamimashiki-gun, Japan). IC_{50} values were obtained using the Logit method and determined from the results of at least 3 independent tests. The relative resistance factor (RF) to each drug was calculated as the ratio of the IC_{50} value of HL-60/MX2 cells to that of HL-60 cells.

Topo I-mediated supercoiled PBR322 relaxation

DNA relaxation assays were based on a previously reported procedure[15]. The reaction buffer contained 10 mmol/L Tris-HCl (pH 7.9), 50 mmol/L KCl, 50 mmol/L NaCl, 5 mmol/L $MgCl_2$, 0.1 mmol/L EDTA, 15 mg/mL bovine serum albumin (BSA), 12.5 μg/mL supercoiled pBR322 for the Topo I assay and 0.01 units/μL of Topo I (TopoGEN, Port Orange, FL, USA). Relaxation was employed at 37 °C for 15 min and stopped via the addition of 2 μL of 10% SDS. Electrophoresis was carried out on a 1% agarose gel in TAE buffer (40 mmol/L Tris base, 40 mmol/L acetate acid, and 1 mmol/L EDTA) at 4 V/cm for 1 h. DNA bands were stained with 0.5 mg/mL of GelRed for 15 min and photographed using a GELDOC XR^+ (Imagelab) (Bio-Rad, CA, USA).

DNA Topo II assays

DNA Topo II activity was assessed via supercoiled pBR322

DNA relaxation and kDNA decatenation assays[15, 16]. The reaction buffer contained 50 mmol/L Tris-HCl (pH 8.0), 150 mmol/L NaCl, 10 mmol/L $MgCl_2$, 2 mmol/L ATP, 0.5 mmol/L dithiothreitol (DTT), 12.5 μg/mL supercoiled pBR322 DNA (Thermo Scientific, Beijing, China) or 20 μg/mL kDNA (TopoGEN, Port Orange, FL, USA), 1 unit of Topo II α (Topogen), and the indicated concentrations of compounds in a total volume of 20 μL. After incubation at 37 °C for 30 min, the reaction was terminated via addition of 2 μL of 10% SDS. The DNA samples were subjected to electrophoresis and photographed under the same conditions as described for the Topo I- and Topo II-mediated supercoiled PBR322 relaxation.

H_2O_2 and $O_2^{\cdot-}$ measurement

Accumulation of intracellular H_2O_2 and $O_2^{\cdot-}$ was detected with the DCFH-DA and HE probes, respectively, as described previously[17]. Briefly, after treatment, the cells were labeled with 10 μmol/L HE or 10 μmol/L DCFH-DA for 30 min at 37 °C in a humidified atmosphere at 5% CO_2. The labeled cells were washed twice and suspended with PBS. To quantify H_2O_2 and $O_2^{\cdot-}$, the fluorescence intensity was measured via flow cytometry (FACSCalibur, BD Biosciences, San Jose, CA, USA).

GSH measurement

Cellular GSH levels were measured using a Glutathione Assay Kit (Beyotime). Briefly, after treatment, the cells were harvested and quickly lysed via freeze/thawing twice. The cells were then centrifuged at 10 000×*g* for 10 min at 4 °C according to the manufacturer's instructions. The supernatant was mixed with 10 mmol/L 5,5′-dithio-bis (2-nitrobenzoic acid) (DTNB), and the GSH levels were measured via the glutathione reductase recycle assay. The optical density at 405 nm was read using a VERSAmax microplate spectrophotometer (Molecular Devices, Sunnyvale, CA, USA), and the GSH concentrations were calculated against a standard curve.

SOD measurement

Cellular SOD levels were measured using Total Superoxide Dismutase Assay Kit with WST-8 (Beyotime). Briefly, after treatment, the cells were harvested and washed with PBS twice and then thoroughly homogenized with a glass homogenizer. The homogenate was centrifuged at 4 °C according to the manufacturer's instructions. SOD levels were assessed with WST-8 and xanthine oxidase assay. The optical density at 450 nm was read using a VERSAmax microplate spectrophotometer (Molecular Devices).

Propidium iodide staining for flow cytometry

HL-60 cells (5×10^5/mL) were seeded into 6-well plates and treated with gradient concentrations of the compounds at 37 °C for 72 h. The cells were harvested and washed with PBS and then fixed with pre-cooled 70% ethanol at -20 °C for 2 h. The cell pellets were suspended in PBS containing 20 μg/mL RNase A and 20 μg/mL propidium iodide (Sigma) at room temperature for 30 min. The cells were then analyzed using a FACSCalibur cytometer (BD Biosciences), and the percentage of cells in each cell cycle phase was calculated using the CELLQUEST and ModFit LT software packages.

Western blot analysis

Treated cells were washed with cold PBS and lysed in RIPA buffer. Equal amounts of protein were separated on SDS-PAGE, transferred to a nitrocellulose membrane (Thermo Scientific, Franklin, MA, USA), blocked with 5% (*w/v*) milk in TBST, and probed with antibodies against caspase 3, caspase 8, caspase 9, PARP (Cell Signaling, Danvers, MA, USA), γ-H2AX (Santa Cruz Biotechnology, CA,USA), and GAPDH (Epitomics, CA, USA). The data shown are typical results obtained from three independent experiments.

Statistical analysis

The data are presented as the mean values±SD from triplicate samples of at least three independent experiments. Statistical significance was analyzed by two-tailed Student's *t*-test. *P* values<0.05 were considered statistically significant.

Results

G226 inhibits cell proliferation

G226 cytotoxicity was evaluated in a panel of human cancer cell lines. As shown in Figure 2, G226 displayed potent cytotoxicity against these cell lines. G226 displayed stronger cytotoxicity than ADR, with an exception for NCI-H460, and the mean IC_{50} for all 9 tested tumor cell lines was 92.7 nmol/L, which was also stronger than that of ADR (232.5 nmol/L). For the sensitive cell lines, such as HL-60, the IC_{50} was 14.3 nmol/L.

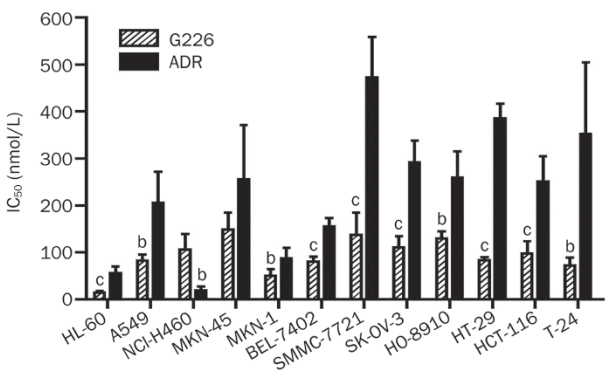

Figure 2. Cytotoxicity of G226 against human tumor cells. Cells in 96-well plates were treated with gradient concentrations of compounds at 37 °C for 72 h. The cell proliferation assay was performed using sulforhodamine B and CCK-8. Mean±SD. *n*=3. $^bP<0.05$, $^cP<0.01$ compared with the DMSO group.

G226 inhibits Topo II activity

First, we assessed the effect of G226 on the catalytic activity of Topo II by evaluating the enzyme-mediated negatively supercoiled pBR322 relaxation. As shown in Figure 3A, G226 displayed significant inhibition of this reaction in a concentration-

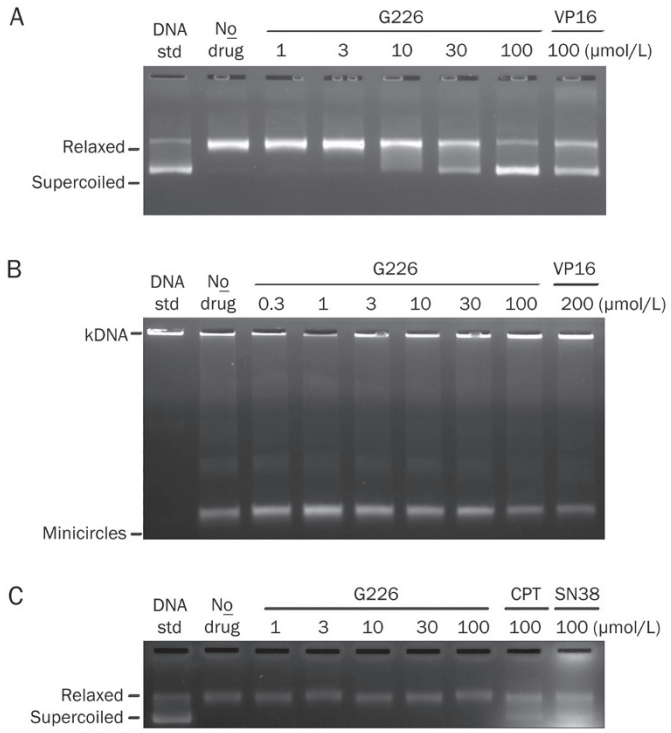

Figure 3. G226 inhibited the activity of Topo II. G226 inhibited Topo II-mediated supercoiled pBR322 relaxation (A) and Topo II-mediated kDNA decatenation (B) but had no effect on Topo I-mediated supercoiled pBR322 relaxation (C).

dependent manner. Accordingly, 10 μmol/L G226 began to inhibit the activity of Topo II, and as the concentration reached 100 μmol/L, G226 rendered most of the pBR322 into supercoiled state. Likewise, 100 μmol/L VP16 displayed a similar effect in suppressing the relaxation activity of Topo II, which was comparable to 30 μmol/L G226. These observations suggest that G226 exerts a stronger inhibitory effect on Topo II relaxation activity than VP16. To further corroborate the effect of G226 on Topo II, a specific Topo II-mediated kDNA decatenation was carried out. Similarly, the capacity to decatenate kDNA with Topo II was reduced in a dose-dependent manner in the presence of G226, and 100 μmol/L G226 forced the kDNA minicircles back to gel aperture as did 200 μmol/L VP16, thereby indicating that G226 completely restrained Topo II activity (Figure 3B).

A supercoiled pBR322 relaxation assay was then executed to test whether G226 could inhibit the catalytic activity of Topo I. The results revealed that 100 μmol/L CPT or SN38 almost completely inhibited the relaxation activity of Topo I. However, G226 failed to show any effect on Topo I (Figure 3C).

G226 induces DNA damage and apoptosis

Phosphorylated-H2AX (γ-H2AX) has become the gold standard for the detection of DNA double strand breaks (DSBs), as it is an extremely sensitive and specific indicator of DNA DSBs, specifically, one γ-H2AX focus correlates to one DSB[18, 19]. As Topo II is well known to efficiently cause DSBs, we further examined whether G226 could induce DNA DSBs. As shown in Figure 4A, γ-H2AX levels were elevated in G226-treated HL-60 cells for 1 h in a concentration-dependent manner. Furthermore, 250 nmol/L G226 significantly enhanced the levels of γ-H2AX, whereas 2 μmol/L G226 induced extremely high levels.

DNA damage always leads to a halt in proliferation owing to apoptosis or cell cycle arrest. To investigate the cell cycle distribution elicited by G226, flow cytometry was performed. G226 induced G_1 arrest in a dose-dependent manner (Figure 4B), whereas 300 nmol/L VP16 and 100 nmol/L ADR arrested HL-60 cells in the G_2/M phase. Propidium iodide staining for Sub-G_1 content analysis was also used to characterize the apoptosis process. We found that G226 induced apoptosis in a dose-dependent manner. Approximately 34.8% HL-60 cells were found to be apoptotic following the treatment of G226 at 50 nmol/L for 24 h. And over 50% of HL-60 cells underwent apoptosis at a concentration of 100 nmol/L (Figure 4C).

G226-triggered DNA damage, apoptosis, and cytotoxicity are partially reduced in Topo II-deficient cells

To confirm that Topo II plays an important role in the process of killing cells via G226, we examined Topo II-deficient HL-60/MX2 cells. This cell line is deficient in Topo II, with a reduced nuclear Topo IIα content (a reduction of approximately 2-fold) and a lack of Topo IIβ. These cells exhibit resistance to mitoxantrone and cross-resistance to VP16, VM-26, and other Topo II inhibitors[20]. The IC_{50} values of G226, several validated Topo II inhibitors (VP16, ADR), and Topo I inhibitors (SN38 and CPT) were assessed in both HL-60 and HL-60/MX2 cell lines. Interestingly, G226 only exhibited slightly less cytotoxicity against HL-60/MX2 cells. The results showed that the RF value of G226 was 3.5, which was much lower than those of VP16 (86.9) and ADR (26.4) (Figure 5A). However, there was no significant difference in the IC_{50} values of CPT and SN38 for HL-60 and HL-60/MX2 cells. The RF values of CPT and SN38 were 1.0 and 1.6, respectively.

We further investigated the effects of Topo II in G226-induced DNA damage and apoptosis. As shown in Figure 5B, as observed with CPT and SN38, G226-induced γ-H2AX was also elevated in HL-60/MX2 cells. However, VP16 and ADR did not trigger an increase in γ-H2AX in HL-60/MX2 cells. Furthermore, PARP, a biochemical characteristic of apoptosis, was evaluated upon compound treatment in both cell lines (Figure 5C). VP16 and ADR only induced PARP cleavage in HL-60 cells; however, G226-triggered PARP cleavage was observed in both cell lines. These findings further supported the hypothesis that Topo II was not crucial for G226-induced cellular DNA damage, apoptosis, and cytotoxicity.

G226 drives ROS generation

As oxidative stress is another inducer of cancer cell DNA damage and apoptosis, we investigated the effect of G226 on intracellular ROS. DCFH-DA and HE are cell-permeable non-fluorescent probes that readily diffuse into cells, which are oxidized by H_2O_2 and $O_2^{\cdot-}$ to highly fluorescent DCF and

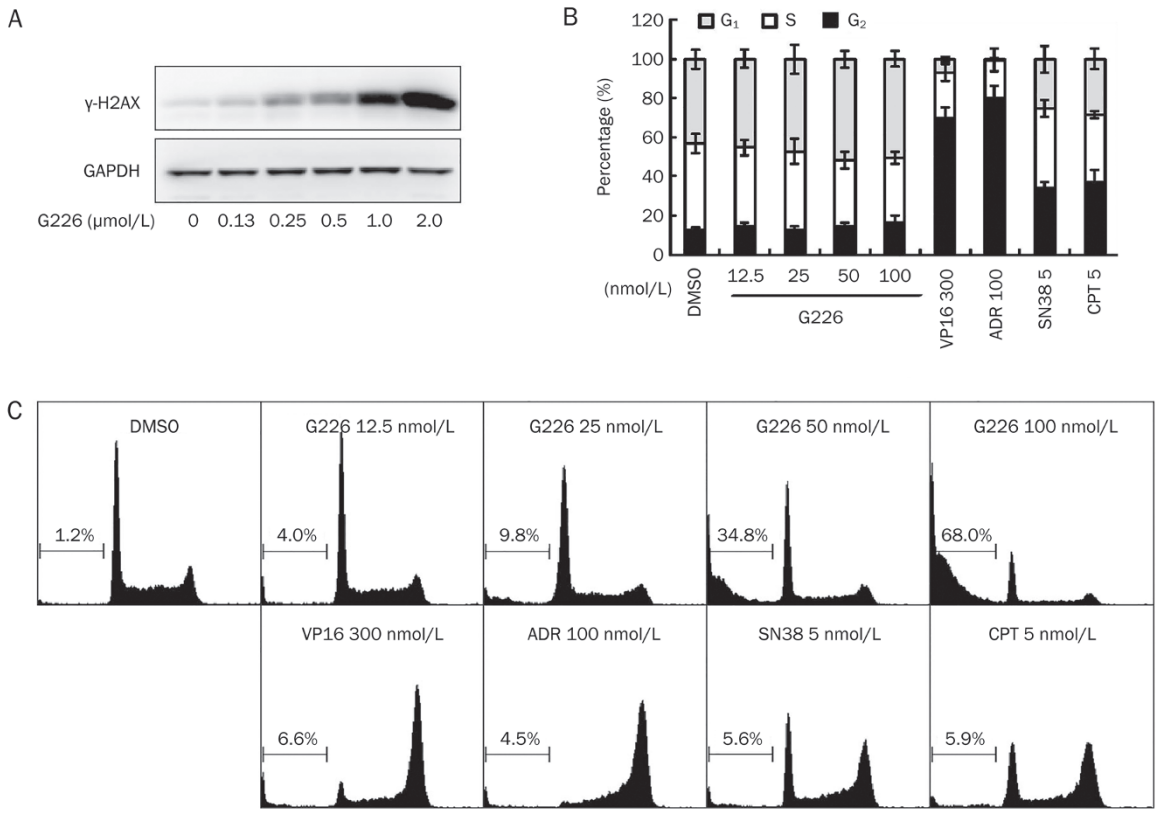

Figure 4. G226 induced DNA DSBs and apoptosis in HL-60 cells. G226 increased the levels of γ-H2AX in 1 h (A), displayed slight G_1 arrest (B) and the increased sub-G_1 cell population (C). The cells were treated with G226, VP16, ADR, SN38, or CPT at the indicated concentrations.

ethidium, respectively. As shown in Figures 6A and 6B, exposure of HL-60 or HL-60/MX2 cells to G226 for 1 h markedly increased intracellular oxidative DCF and ethidium fluorescence intensity, which is proportional to the amount of intracellular ROS. G226 (1 μmol/L) significantly increased the level of H_2O_2 up to 4.3-fold and 3.0-fold of the basal values in HL-60 and HL-60/MX2 cells, respectively. Similarly, 1 μmol/L G226 significantly increased the level of $O_2^{\cdot-}$ up to 3.3-fold and 2.5-fold in HL-60 and HL-60/MX2 cells, respectively. Additionally, G226 also increased the levels of ROS in WILL-1, U-2932, and HT-29 cells (Figures 6C, 6D, and 6E). These results suggest that ROS might contribute to G226-induced DNA damage and apoptosis.

GSH is a major antioxidant in cells and can convert H_2O_2 to H_2O, whereas SOD is superoxide dismutase and a specific scavenger of $O_2^{\cdot-}$ that converts $O_2^{\cdot-}$ to H_2O_2. We aimed to assess whether G226 has a direct impact on intracellular GSH and SOD. Figures 6E and 6F clearly show that G226 had no effect on intracellular GSH and SOD. These results suggest that GSH and SOD are not involved in G226-induced ROS generation.

Antioxidants attenuates G226-mediated DNA damage and apoptosis

NAC, GSH and DTT are ROS scavengers that have been widely used to define the function of ROS in numerous biological and pathological processes. To investigate whether ROS generation is responsible for G226-induced DNA damage and apoptosis, we also used these antioxidants. Pretreatment with NAC, GSH, or DTT completely suppressed the G226-induced increase in ROS levels in HL-60, HL-60/MX2, and HT-29 cells, including H_2O_2 and $O_2^{\cdot-}$ (Figures 7A–7F).

Next, the correlation between increased ROS levels and G226-induced DSBs was analyzed via pretreatment of cells with these antioxidants prior to G226 treatment. The protective effect of the antioxidants was reflected more clearly by γ-H2AX expression, which revealed that phosphorylation of H2AX in the antioxidant-pretreated groups all displayed decreasing trends compared with the G226-only-treated groups (Figure 7G). Furthermore, the levels of cleavage of PARP, caspase 8 and caspase 3 were assessed to investigate the effect of intracellular ROS on G226-mediated apoptosis. G226 dose-dependently induced pro-caspase 8, pro-caspase 3, and PARP cleavage in both HL-60 and HL-60/MX2 cells. Furthermore, pretreatment with 2 mmol/L GSH or 4 mmol/L NAC markedly antagonized the effect of G226 (Figure 7H). Additionally, the flow cytometry data further confirmed that apoptosis induced by G226 was nearly abrogated by pretreatment with 2 mmol/L GSH or 4 mmol/L NAC (Figure 7I). Taken together, these results indicate that G226-mediated ROS production contributed to G226-induced DNA damage and apoptosis.

A

IC_{50} (mean±SD)	Compounds G226 (nmol/L)	VP16 (μmol/L)	ADR (μmol/L)	SN38 (nmol/L)	CPT (nmol/L)
HL-60	14.3±0.5	0.13±0.03	0.053±0.008	6.3±3.3	15.0±2.8
HL-60/MX2	50.0±14.8	11.3±3.6	1.4±0.4	9.8±4.6	15.0±5.8
RF	3.5	86.9	26.4	1.6	1.0

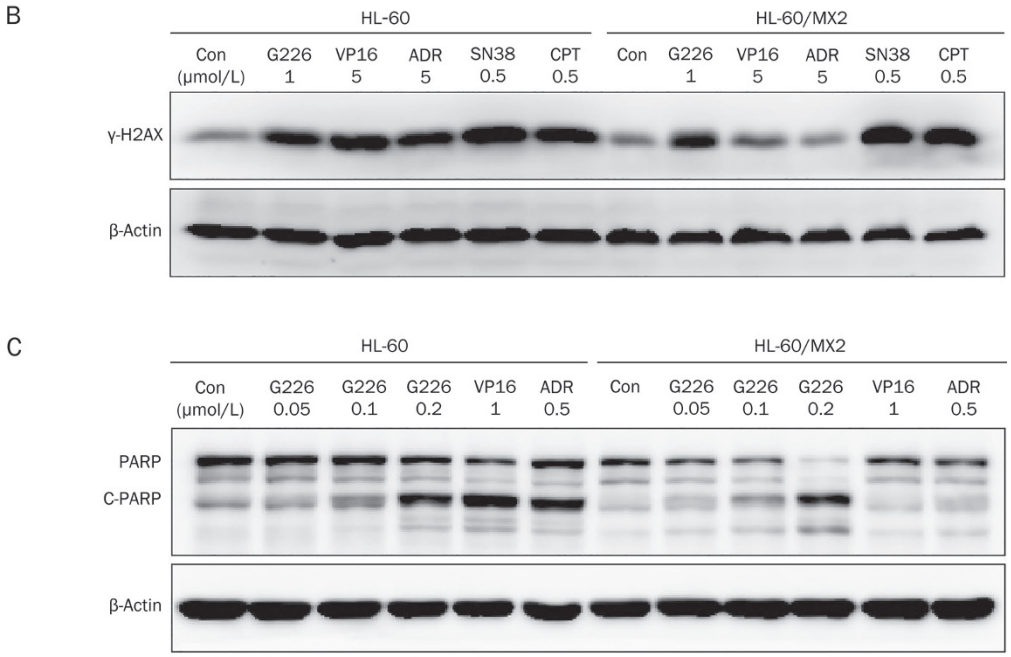

Figure 5. G226-triggered DNA damage, apoptosis, and cytotoxicity were partially reduced in Topo II-deficient HL-60/MX2 cells. (A) G226 inhibited Topo II-deficient HL-60/MX2 cell proliferation. Three separate experiments were carried out to determine the IC_{50} value, which is expressed as the mean±SD. A resistance factor (RF) comparison of G226, VP16, ADR, SN38, and CPT in HL-60 and HL-60/MX2 cells is shown. (B) G226, SN38, and CPT increased the levels of γ-H2AX in both of HL-60 and HL-60/MX2 cells. (C) G226 induced PARP cleavage with increasing concentration in both HL-60 and HL-60/MX2 cells.

GSH reverses G226-mediated Topo II inhibition

To investigate whether GSH affects G226-induced Topo II inhibition, a pBR322 DNA relaxation assay was performed. As shown in Figure 8, G226 significantly suppressed the relaxation of negatively supercoiled pBR322 DNA mediated by Topo II. Importantly, the addition of GSH remarkably reversed G226-induced Topo II inhibition in a dose-dependent manner but had no effect on VP16-induced Topo II inhibition.

Discussion

G226 is a novel ETP analogue, which possesses potent activity against malignant tumor cells and induces apoptosis and autophagy in various human tumor cell lines. It is important to understand the precise mechanisms of G226-induced cancer cell death. Topoisomerase inhibitor is a highly active and widely prescribed antineoplastic drug. There has been continuous interest in studying and developing new anti-Topo agents, and several potential compounds are currently in clinical trial. Recent studies have shown that ETPs inhibit the activity of Topo I and Topo II, such as leptosin F and leptosin C[13]. We found that G226 significantly inhibited Topo II-mediated supercoiled pBR322 relaxation and kDNA decatenation. Additionally, G226 increased the levels of γ-H2AX, resembling other known Topo II poisons. These findings suggest that G226 may target Topo II to inhibit cancer cell growth. Although it is well known that many Topo II-targeted anticancer drugs often cause DNA strand breaks[21], Topo II poisons are not the only ones to induce DNA damage. Indeed, the patterns of DNA breaks induced by Topo II inhibitors are similar to other stimuli such as ROS[22]. We were thus encouraged to address effects of G226-driven Topo II inhibition and understand whether it plays a vital role in G226-mediated DNA damage and apoptosis. Therefore, we examined the HL-60/MX2 cell line, which is deficient in Topo II and exhibits resistance to Topo II inhibitors, such as mitoxantrone, VP16, VM-26, and R16[20, 21]. This cell line also displayed resistance to VP-16 and ADR; the RF values were 86.9 and 26.4, respectively. However, the RF value of G226 was only 3.5. More-

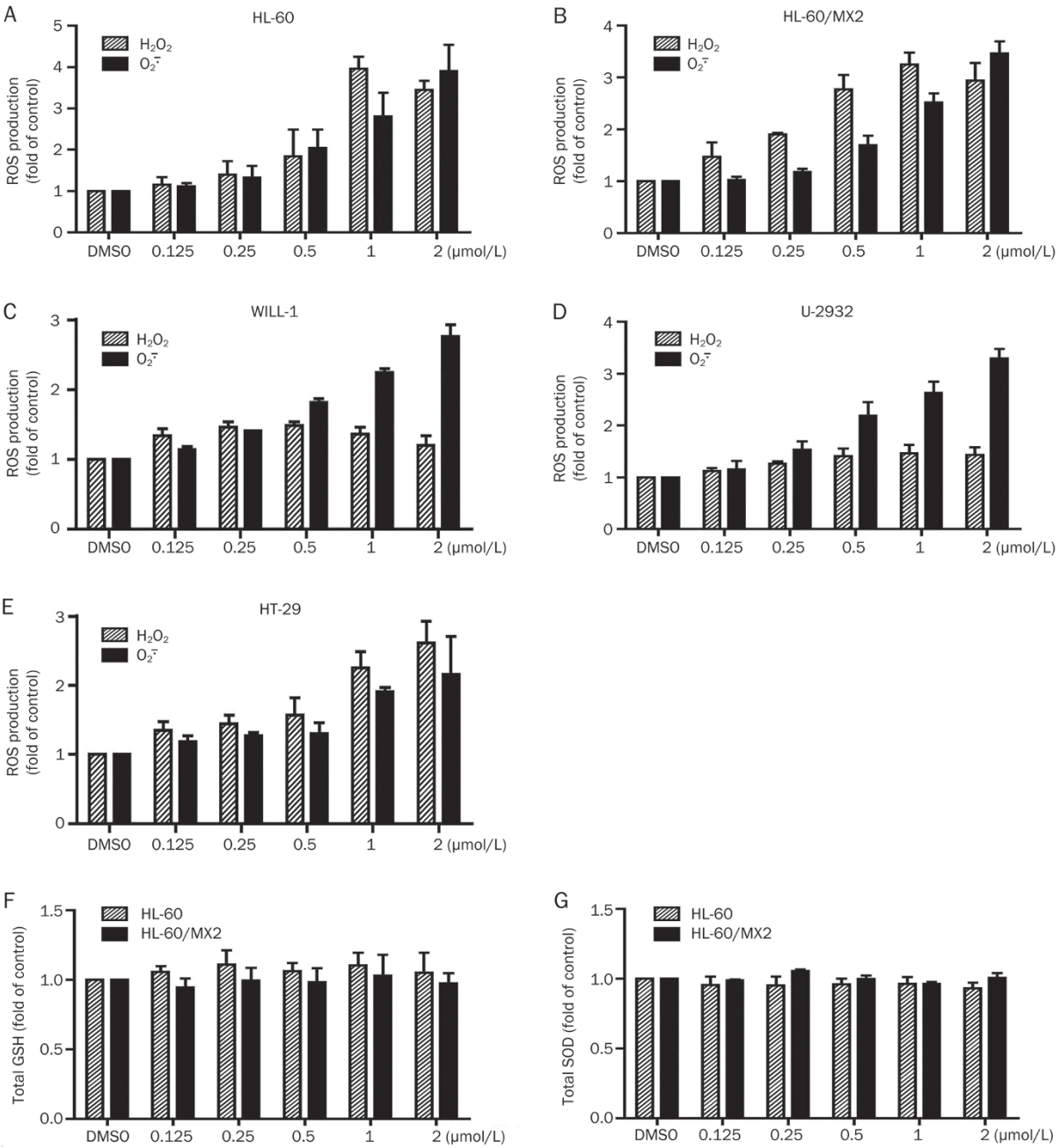

Figure 6. G226 drives intracellular ROS generation. Changes in the levels of intracellular H_2O_2 and $O_2^{\cdot-}$ mediated by exposure to increasing concentrations of G226 for 1 h were detected in HL-60 (A), HL-60/MX2 (B), WILL-1 (C), U-2932 (D), and HT-29 cells (E) via flow cytometry using DCFH-DA or HE as the fluorescent probe. The total levels of intracellular GSH and SOD following exposure to increasing concentrations of G226 for 1 h were detected in HL-60 (F and G).

over, DNA DSB induction, apoptosis activation, and cell-killing ability of G226 were not evidently reduced in HL-60/MX2 cells. These observations strongly suggest that in addition to Topo II, other important mechanisms must be involved in the anti-tumor activities of G226.

Although ROS, such as hydrogen peroxide (H_2O_2), hydroxyl radicals (HO·), and superoxide anions ($O_2^{\cdot-}$), are natural byproducts of the normal metabolism of oxygen and play an important role in cell signaling and homeostasis[23], they have been shown to damage chromosomal DNA and other cellular components, thereby resulting in DNA degradation, protein denaturation, and lipid peroxidation[22]. Increased ROS levels due to environmental stress induce DNA damage and thus enhance tumor development[24]. Much emphasis has been focused on antioxidants to battle the toxic effects of ROS. However, accumulating evidence has highlighted the beneficial functions of ROS, including their application as chemotherapeutic agents to cure human diseases. Many anti-tumor

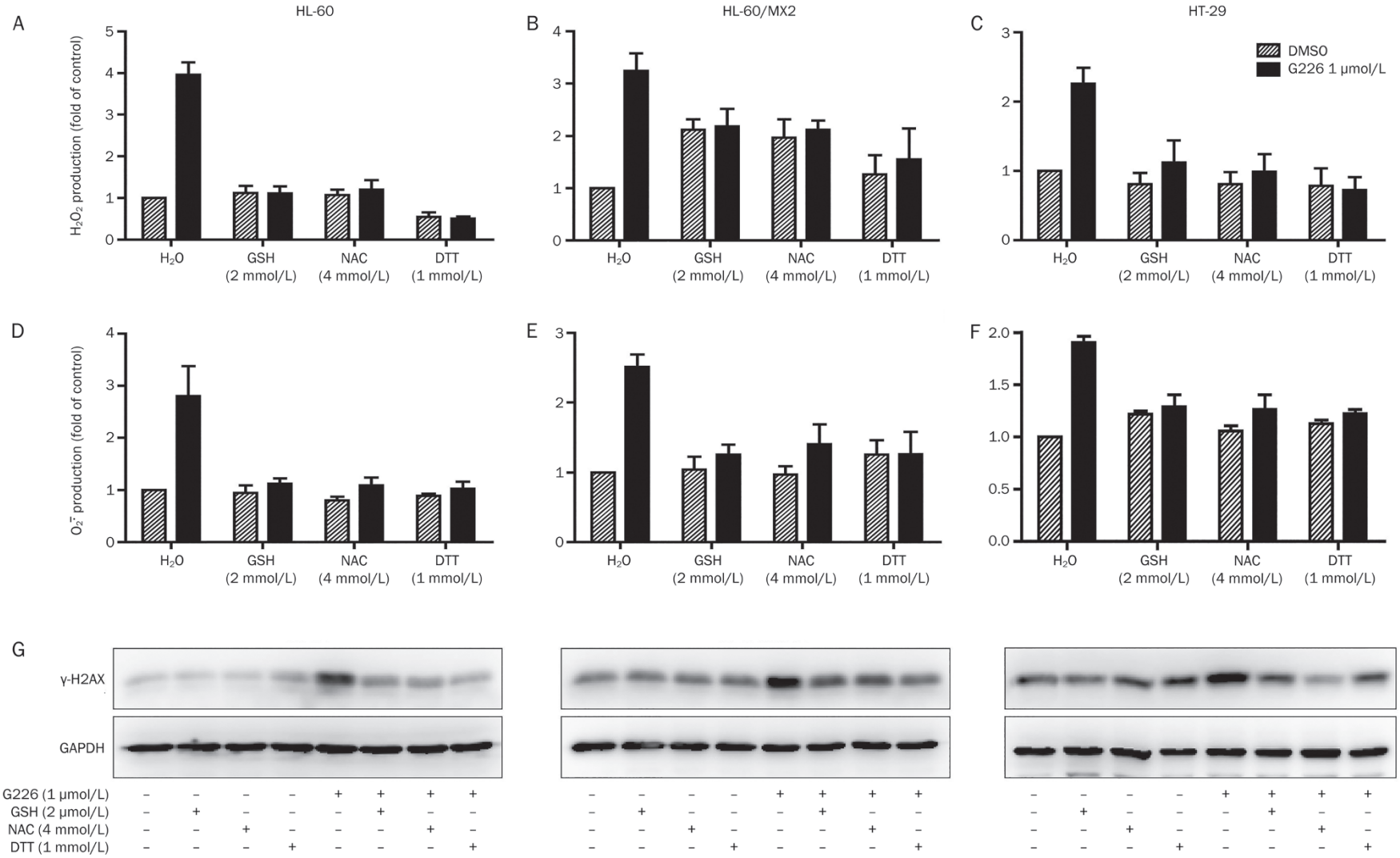

Figure 7A–7G. GSH, NAC, and DTT suppressed ROS generation, DNA damage and apoptosis mediated by G226. G226-mediated ROS generation (A–F) and the levels of γ-H2AX (G) were attenuated by GSH, NAC, and DTT in HL-60, HL-60/MX2, and HT-29 cells.

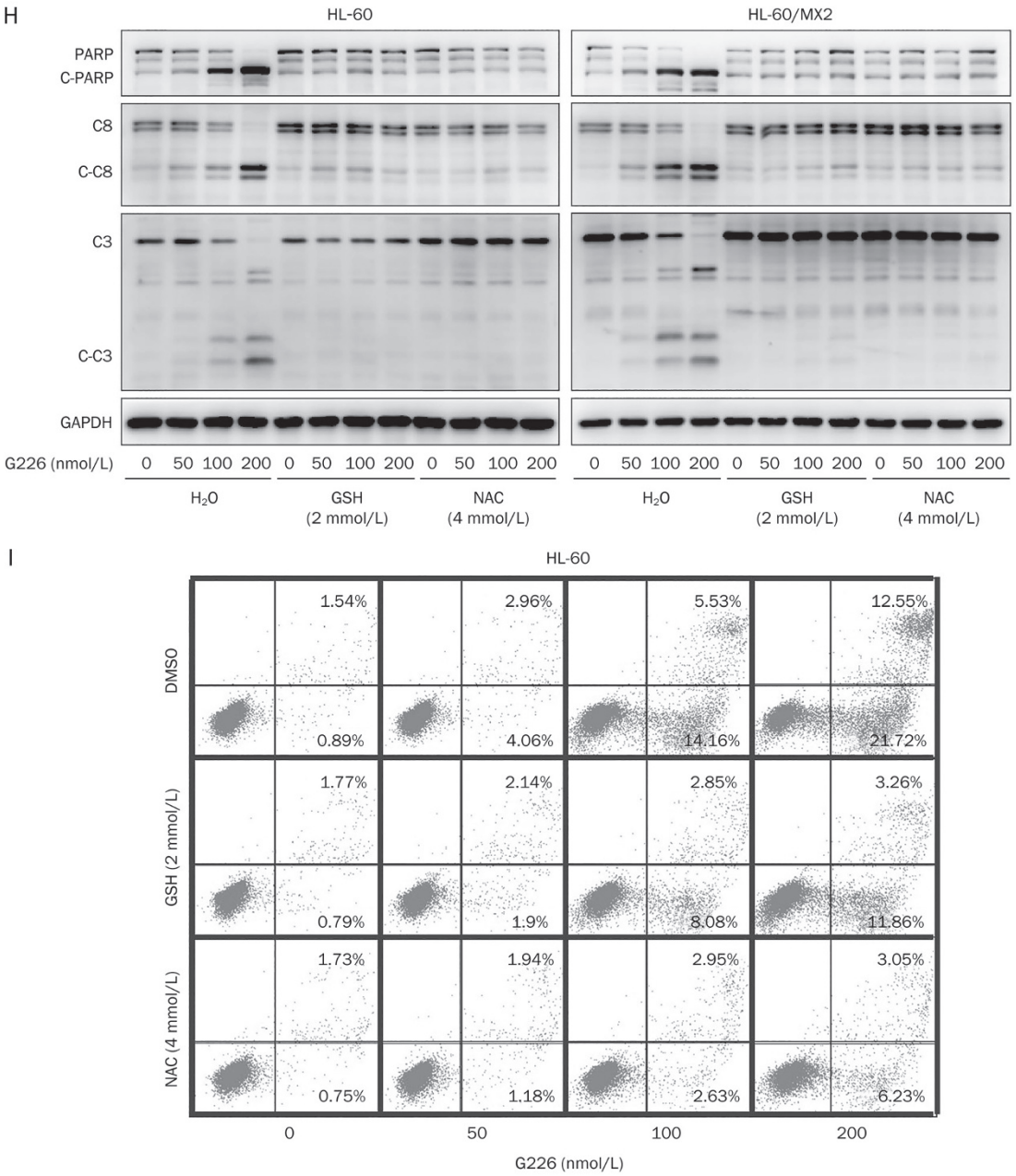

Figure 7H–7I. Cleavage of pro-caspase 8, pro-caspase 3, and PARP (H) was inhibited by GSH and NAC in both HL-60 and HL-60/MX2 cells. GSH and NAC also reversed G226-mediated apoptosis (I) in HL-60 cells.

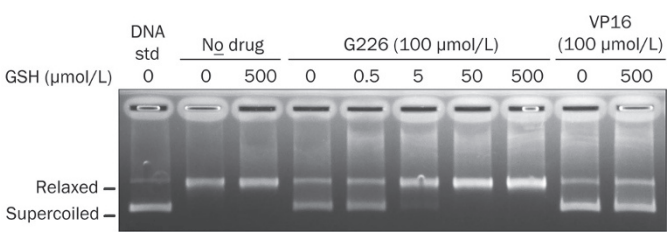

Figure 8. GSH reversed G226-mediated Topo II inhibition.

drugs have been developed in this context to generate ROS and cause oxidative stress-induced apoptosis in cancer cells, such as doxorubicin, salvicine, arsenic, electromagnetic radiation[17, 25–27]. Some of these drugs exhibit anti-tumor activity via ROS-dependent activation of apoptotic cell death, thereby suggesting the potential application of ROS as anti-tumor agents. Thus, a unique anticancer strategy termed "oxidation therapy" has been developed by inducing cytotoxic oxystress for cancer treatment. This goal was achieved primarily via two methods, inducing the generation of ROS directly in solid tumors and inhibiting the antioxidative enzyme (defense) system of tumor

cells[28]. In this study, we verified that G226 could quickly induce ROS generation in cancer cells. The addition of antioxidants, such as NAC, GSH, and DTT, all effectively decreased G226-induced ROS enhancement and the subsequent DNA DSBs, which was consistent with reports that the antioxidant GSH reversed salvicine-induced DNA damage and apoptosis via ROS generation. However, this agent did not deplete intracellular levels of GSH and SOD.

It is believed that the toxicity of ETP is mediated via conjugation to proteins with susceptible thiol residues[11]. Therefore, we hypothesized that G226 is capable of modifying thiol groups of Topo II cysteine residues. We confirmed that G226 directly reacts with Topo II and inhibits the activity of Topo II in cell-free system. In a supercoiled pBR322 relaxation assay, thiol antioxidant GSH remarkably reversed G226-induced Topo IIα inhibition. However, GSH had no effect on VP-16-induced Topo II inhibition. We thus make a bold presumption that G226, at least in part, has the potential to modify the thiol groups of Topo II.

In summary, we have demonstrated that G226 triggers DNA double strand breaks and apoptosis via ROS generation and functions as a novel Topo II inhibitor.

Acknowledgements

The project was supported by the National Natural Science Foundation of China (81273545) and the National Basic Research Program Grant of China (2013CB932503).

Author contribution

Jian DING, Yi CHEN, Qiao-jun HE, Peng-xing HE, and Jie ZHANG designed the research project; Yong-sheng CHE provided the G226 compound; Peng-xing HE and Jie ZHANG performed the experiments, analyzed the results and wrote the manuscript; Yi CHEN and Jian DING revised the paper.

References

1 Wang JC. Cellular roles of DNA topoisomerases: a molecular perspective. Nat Rev Mol Cell Biol 2002; 3: 430–40.
2 Nitiss JL. Targeting DNA topoisomerase II in cancer chemotherapy. Nat Rev Cancer 2009; 9: 338–50.
3 Shi ZY, Li YQ, Kang YH, Hu GQ, Huang-fu CS, Deng JB, *et al*. Piperonal ciprofloxacin hydrazone induces growth arrest and apoptosis of human hepatocarcinoma SMMC-7721 cells. Acta Pharmacol Sin 2012; 33: 271–8.
4 Rahal A, Kumar A, Singh V, Yadav B, Tiwari R, Chakraborty S, *et al*. Oxidative stress, prooxidants, and antioxidants: the interplay. Biomed Res Int 2014; 2014: 761264.
5 Hancock JT, Desikan R, Neill SJ. Role of reactive oxygen species in cell signalling pathways. Biochem Soc Trans 2001; 29: 345–50.
6 Durackova Z. Some current insights into oxidative stress. Physiol Res 2010; 59: 459–69.
7 Hussain SP, Hofseth LJ, Harris CC. Radical causes of cancer. Nat Rev Cancer 2003; 3: 276–85.
8 Martindale JL, Holbrook NJ. Cellular response to oxidative stress: signaling for suicide and survival. J Cell Physiol 2002; 192: 1–15.
9 Yi J, Yang J, He R, Gao F, Sang H, Tang X, *et al*. Emodin enhances arsenic trioxide-induced apoptosis via generation of reactive oxygen species and inhibition of survival signaling. Cancer Res 2004; 64: 108–16.
10 Yang LJ, Chen Y. New targets for the antitumor activity of gambogic acid in hematologic malignancies. Acta Pharmacol Sin 2013; 34: 191–8.
11 Gardiner DM, Waring P, Howlett BJ. The epipolythiodioxopiperazine (ETP) class of fungal toxins: distribution, mode of action, functions and biosynthesis. Microbiology 2005; 151: 1021–32.
12 Son BW, Jensen PR, Kauffman CA, Fenical W. New cytotoxic epidithiodioxopiperazines related to verticillin A from a marine isolate of the fungus penicillium. Nat Prod Lett 1999; 13: 213–22.
13 Yanagihara M, Sasaki-Takahashi N, Sugahara T, Yamamoto S, Shinomi M, Yamashita I, *et al*. Leptosins isolated from marine fungus Leptoshaeria species inhibit DNA topoisomerases I and/or II and induce apoptosis by inactivation of Akt/protein kinase B. Cancer Sci 2005; 96: 816–24.
14 Chen Y, Zhang YX, Li MH, Zhao WM, Shi YH, Miao ZH, *et al*. Anti-angiogenic activity of 11,11′-dideoxyverticillin, a natural product isolated from the fungus Shiraia bambusicola. Biochem Biophys Res Commun 2005; 329: 1334–42.
15 Tanabe K, Ikegami Y, Ishida R, Andoh T. Inhibition of topoisomerase II by antitumor agents bis(2,6-dioxopiperazine) derivatives. Cancer Res 1991; 51: 4903–8.
16 Osheroff N, Shelton ER, Brutlag DL. DNA topoisomerase II from Drosophila melanogaster. Relaxation of supercoiled DNA. J Biol Chem 1983; 258: 9536–43.
17 Cai YJ, Lu JJ, Zhu H, Xie H, Huang M, Lin LP, *et al*. Salvicine triggers DNA double-strand breaks and apoptosis by GSH-depletion-driven H_2O_2 generation and topoisomerase II inhibition. Free Radic Biol Med 2008; 45: 627–35.
18 Sedelnikova OA, Rogakou EP, Panyutin IG, Bonner WM. Quantitative detection of (125)IdU-induced DNA double-strand breaks with gamma-H2AX antibody. Radiat Res 2002; 158: 486–92.
19 Takahashi A, Ohnishi T. Does gammaH2AX foci formation depend on the presence of DNA double strand breaks? Cancer Lett 2005; 229: 171–9.
20 Harker WG, Slade DL, Drake FH, Parr RL. Mitoxantrone resistance in HL-60 leukemia cells: reduced nuclear topoisomerase II catalytic activity and drug-induced DNA cleavage in association with reduced expression of the topoisomerase II beta isoform. Biochemistry 1991; 30: 9953–61.
21 Zhu H, Huang M, Yang F, Chen Y, Miao ZH, Qian XH, *et al*. R16, a novel amonafide analogue, induces apoptosis and G_2-M arrest via poisoning topoisomerase II. Mol Cancer Ther 2007; 6: 484–95.
22 Higuchi Y. Chromosomal DNA fragmentation in apoptosis and necrosis induced by oxidative stress. Biochem Pharmacol 2003; 66: 1527–35.
23 Sena LA, Chandel NS. Physiological roles of mitochondrial reactive oxygen species. Molecular Cell 2012; 48: 158–67.
24 Alfadda AA, Sallam RM. Reactive oxygen species in health and disease. J Biomed Biotechnol 2012; 2012: 936486.
25 Kotamraju S, Kalivendi SV, Konorev E, Chitambar CR, Joseph J, Kalyanaraman B. Oxidant-induced iron signaling in Doxorubicin-mediated apoptosis. Methods Enzymol 2004; 378: 362–82.
26 Bhattacharjee P, Banerjee M, Giri AK. Role of genomic instability in arsenic-induced carcinogenicity. A review. Environ Int 2013; 53: 29–40.
27 Hou Q, Wang M, Wu S, Ma X, An G, Liu H, *et al*. Oxidative changes and apoptosis induced by 1800-MHz electromagnetic radiation in NIH/3T3 cells. Electromagn Biol Med 2014 Mar 25. [Epub ahead of print].
28 Fang J, Nakamura H, Iyer AK. Tumor-targeted induction of oxystress for cancer therapy. J Drug Target 2007; 15: 475–86.